

Multi-material distributed recycling via Fused granular fabrication: rHDPE and rPET case of study

Catalina Suescun Gonzalez¹, Hakim Boudaoud¹, Cécile Nouvel², Fabio A. Cruz Sanchez¹, Joshua Pearce³

¹Université de Lorraine – ERPI – F-54000, Nancy, France

²Université de Lorraine – LGPI – F-54000, Nancy, France

³Western University, Department of Electrical & Computer Engineering, Canada, London

Abstract

The high volume of plastic waste and the extremely low recycling rate has created a serious challenge worldwide. Local distributed recycling coupled to additive manufacturing (DRAM) offers a solution by economically incentivizing local recycling. A new DRAM technology capable of processing large quantities of plastic waste quickly is fused granular fabrication (FGF), where solid shredded plastic waste can be reused directly as 3D printing feedstock. This study presents an experimental assessment of multi-material recycling printability, using two of the most common thermoplastics in the beverage industry polyethylene terephthalate (PET) and high-density polyethylene (HDPE) and the feasibility of mixing PET and HDPE to be used as a feedstock material for large-scale 3-D printing. After the material collection, shredding, and cleaning its characterization, and optimization of parameters for 3D printing was performed. Results showed the feasibility of printing a large object from rPET/rHDPE flakes reducing the production cost up to 88%.

Acronyms

Acronym	Definition
ABS	Poly(acrylonitrile butadiene styrene)
AM	Additive Manufacturing
DRAM	Distributed recycling via additive manufacturing
DSC	Melt flow index
FDM	Fused deposition modeling
FFF	Fused filament fabrication
FGF	Fused granular fabrication
FPF	Fused particle fabrication
FTIR	Differential scanning calorimetry
HDPE	High-density polyethylene
MFI	Virgin or commercial Poly(ethylene terephthalate)
PC	Polycarbonate
PET	Poly(ethylene terephthalate)
PLA	Poly(lactic acid)
PP	Polypropylene
PSO	Particle swarm optimization
PS	Polystyrene
SEBS	Poly (styrene-block-ethene-co-butene-block-styrene)
Tg	Degree of crystallization
pBC	Glass temperature
rHDPE	Recycled High-density Polyethylene
rPET90//rHDPE10	Recycled Bottle-Cap (Cristaline bottle shredded without separation)
rPET	Recycled Poly(ethylene) terephthalate
vPET	Printed Bottle-Cap
NA	Fourier-transform infrared spectroscopy

1 Introduction

- ¹ The disposal of plastic waste is one of the most challenging current environmental concerns
² given its systemic complexity ([Evode et al., 2021](#)). The mass of micro- / meso- plastics in the
³ oceans are expected to exceed the mass of the global stock of fish by 2050 ([MacArthur, 2017](#)).
⁴ More critically, the global plastic annual production is expected to reach 1100 metric tons
⁵ by the same year ([Geyer, 2020](#)). The societal awareness on plastic recycling have received
⁶ substantial attention by scientific, policymaker and general public ([Soares et al., 2021](#)). Un-
⁷ fortunately, the statistical analysis on the centralized recycling process proves that it has
⁸ been largely ineffective ([Siltaloppi and Jähi, 2021](#)) as only 9% of the plastic that has been
⁹ produced has been recycled from the total stock produced since 1950 ([Geyer et al., 2017](#)).
¹⁰ Therefore, it remains an open challenge to identify alternatives to valorize discarded plastic

11 material.

12 Distributed recycling and additive manufacturing (DRAM), is an innovative technical ap-
13 proach to recycle plastic wastes (Cruz Sanchez et al., 2020; Dertinger et al., 2020). DRAM
14 was first practiced with recyclebots, which are waste plastic extruders that made filament
15 for conventional fused filament-based 3-D printers (Baechler et al., 2013; Woern et al., 2018;
16 Zhong and Pearce, 2018). Past research demonstrated that using distributed recycling fits
17 into the circular economy paradigm (Despeisse et al., 2017; Ford and Despeisse, 2016); where
18 consumers directly recycle their own waste into consumer products from open source designs,
19 from toys for children (Petersen et al., 2017) to adaptive aids for those with arthritis (Gallup
20 et al., 2018). Distributed manufacturing is now in wide use (Pearce and Qian, 2022). In this
21 way DRAM-based recycling is done in a closed loop supply chain network (Santander et al.,
22 2020). This type of recycling aims to reduce the environmental impact by the reduction of
23 the transportation from the waste source to recycling facilities (M. A. Kreiger et al., 2014).
24 In that sense, it aims to propose innovative closed-loop strategies using waste materials as
25 raw resources (Romani et al., 2021).

26 Fused filament fabrication (FFF, which is also known as Fused Deposition Modelling –FDM©–
27) is the most-widespread and established extrusion-based AM technology due to the open
28 source proliferation from the self-replicating rapid prototyper (RepRap) project (Bowyer,
29 2014; Jones et al., 2011; Sells et al., 2009). This is due to its simplicity, versatility, low-
30 cost, and ability in the construction of geometrically complex objects in the industrial and
31 prosumer domains (Romani et al., 2021). Indeed, the open-source 3-D approach for 3-D
32 printers has enabled the technology to evolve in a radical manner for manufacturing and
33 prototyping adding value to the recycled material (Cruz Sanchez et al., 2020). There are
34 large efforts to find sustainable feedstocks for 3-D printing Pakkanen et al. (2017a). Several
35 studies in the literature have increase the spectrum of recycled filament materials such as
36 PLA (Anderson, 2017; Cruz Sanchez et al., 2017), ABS (Mohammed et al., 2017b, 2017a),
37 PET (Vaucher et al., 2022; Zander et al., 2018), HDPE (Baechler et al., 2013; Chong et al.,
38 2017; Mohammed et al., 2017b) PC (Gaikwad et al., 2018). In fact, using a comparative life

39 cycle assessment in a low density population case study of Michigan, USA, M. a. Kreiger et al.
40 (2014) argued that about of 100 billion MJ of energy per year could be saved in a distributed
41 approach, for the 984 million pounds of HDPE that are recycled in the U.S. There is thus
42 considerable evidence that DRAM can reduce the energy consumption and greenhouse gases
43 of the manufacturing processes.

44 Most DRAM studies have been using mono-material for the fabrication of feedstock for
45 FFF. There are, however, several examples of mixed materials including wood waste and
46 recycled plastic (Löschke et al., 2019; Pringle et al., 2018) and textile fibers and recycled
47 plastic (Carrete et al., 2021). Recently, Zander et al. (2019) reported the manufacturing
48 of composite filament from recycled PET/PP and PS/PP blending through compatibilizer
49 copolymer such as SEBS. Their results revealed the technical printability of polypropylene
50 blend composite filaments from a thermo-mechanical characterization perspective. Increasing
51 the performance window of blending materials by compatibilization which could be a relevant
52 path for recycling plastics in a local level and isolated areas contexts (e.g. during humanitarian
53 crises (Savonen et al., 2018 ; Corsini et al., 2022 ; Lipsky et al., 2019), supply chain disruptions
54 (Attaran, 2020; Choong et al., 2020 ; Novak and Loy, 2020; Salmi et al., 2020) and/or isolated
55 off-grid situations using solar-powered 3-D printers (Gwamuri et al., 2016 ; King et al., 2014;
56 Mohammed et al., 2018; Wong, 2015)). Likewise, Vaucher et al. (2022) studied the evaluation
57 of the microstructure, mechanical performance, and printing quality of filaments made from
58 rPET and rHDPE varying the wt% of HDPE material from 0 to 10%. They confirmed the
59 increase in the Young's modulus from 1.7 GPa of the pure PET to 2.1 GPa for all the HDPE
60 concentrations. Additionally, the maximum stress of the bends were augmented with high
61 HDPE concentrations. Values were lower than virgin PET filament, yet similar to commercial
62 recycle ones. The addition of rHDPE at higher levels, however, helped to meet the brittle-
63 ductile transition in 15% despite the low interfacial tension of both polymers, allowing the
64 printing of quality parts.

65 While former studies have proven been successful in FFF, a new approach to DRAM is
66 fused granular fabrication (FGF) or fused particle fabrication (FPF), where the material-

67 extrusion AM systems print directly from pellets, granules, flakes, shred or grinder material
68 (Fontana et al., 2022; Woern et al., 2018). In the context of recycling, this could reduce the
69 number of melt/extrusion cycles that degrade the material needed in the filament fabrication
70 process (Cruz Sanchez et al., 2017). The FGF technique opens up the potential of use
71 recycle materials as well as print large-scale objects either with a conventional cartesian 3-D
72 printer (Woern et al., 2018), delta 3-D printer (Grassi et al., 2019) or hangprinter Rattan
73 et al. (2023). Research groups corroborate that plastic waste can be used as feedstock
74 materials for FGF/FPF. Alexandre et al. (2020) assessed the technical and economical
75 dimensions of virgin and shredded PLA printed in a self-modified FGF machine and compared
76 with FFF. The investigation showed that the use of FGF reduced printing cost, time and
77 its mechanical performance was comparable with the obtained using the traditional FFF
78 technique. Likewise, Woern et al. (2018) found comparable properties between PLA, ABS,
79 PP, and PET recycled and virgin materials. Later publications demonstrated the technical
80 and economic feasibility through the printing of complex objects validating the possibility
81 of recycle plastic with FGF in both conventional and common FFF materials (Byard et
82 al., 2019), but also recycle PC (Reich et al., 2019) and rPET (Little et al., 2020.). Few
83 researchers, however, have addressed the problem of the direct printing of recycled multi-
84 materials, which might be a key step forward needed to facilitate the ease of sorting and
85 recycling post-consumer plastic waste materials.

86 This study explores the potential of direct 3-D printing two immiscible polymers commonly
87 used in the beverage sector through a distributed recycling process for its easily implemen-
88 tation operation at the local level. To demonstrate the feasibility of the process, the bottled
89 water plastic most used in France of roughly 90% of PET (body of the bottle) and 10% of
90 HDPE (cap) now called *rPET90//rHDPE10*, is used as a test material. The experimental
91 process of collection, characterization, and printing of the recycled material is described and
92 the results are discussed in the context of widespread DRAM adoption at the community-
93 based level.

94 2 Materials and Methods

95 The methodology presented in Figure 1 outlines the approach adopted to develop the study.
96 The four stages *Material*, *Material preparation*, *Printing process* and *Evaluation* were thor-
97oughly studied in order to control the major processes steps and the technical characterization
98 methods. In the following subsections, each step is explained.

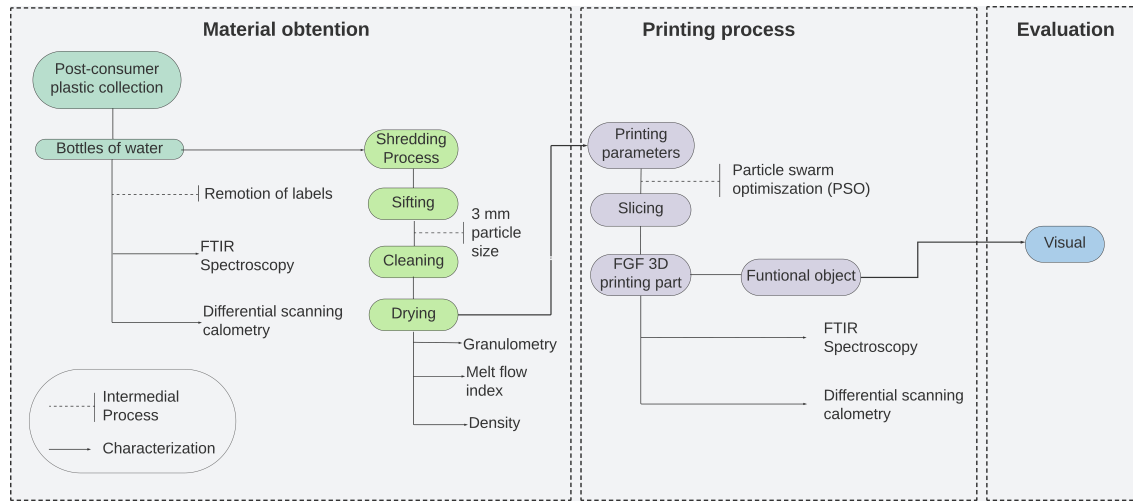


Figure 1: Global framework of the study

99 2.1 Raw material obtention

100 The goal of material stage is the collection and preparation of post-consumer plastic source. In
101 this study, bottles of water coming from the French brand Cristaline was used as a feedstock.
102 The process steps used are shown in Figure 2 a/b. Post-consumer bottles were collected by
103 receptacles placed in partnership schools in Lorraine, France. To convert the complete water
104 bottles with its cap into 3DP feedstock material, the labels were removed before shredding
105 in a cutting mill Retsch MS300 using a 3 mm grid. After shredding, the obtained flakes were
106 sifted with a 1.5 mm, 3 mm, 5 mm sifters for further analysis. Next, flakes were cleaned
107 with hot water in an ultrasonic machine at 60°C for 1h to remove contaminants. Lastly, they
108 were dried in a conventional oven overnight at 80°C (Taghavi et al., 2018; Van de Voorde et
109 al., 2022) to avoid degradation of the material. Washing conditions were the same for all the

110 samples, therefore, the effect of contaminants was not considered. The resultant material is
111 shown in Fig 2.c.



Figure 2: Process steps to prepare the collected material

112 The material composition was calculated as a function of the mass of the bottles and caps
113 separately. The percent (%) of bottle-cap was found to be ~90% rPET (bottle) and ~10%
114 rHDPE (cap). The complete bottle was shredded without separation of both materials thus
115 this percentage is constant for all the samples.

116 2.2 Material preparation and characterization

117 2.2.1 Material particle size analysis -Granulometry-

118 In order to ensure the particle size suitable for printing, the characterization of the granulate
119 particles were developed using the open-source ImageJ software ([ImageJ, 2023](#)). The size
120 characteristics of the particles were evaluated between four different samples; vPET (used as
121 a reference) and the raw material sifted in three different sizes 1.5 mm, 3 mm and 5 mm.

¹²² **2.2.2 Fourier-transform infrared spectroscopy –FTIR-**

¹²³ FTIR spectroscopy was carried out to determine the nature of the bottle and determine
¹²⁴ if there were impurities, plasticizers or additives that could be detected. The analysis were
¹²⁵ made on samples of rPET and rHDPE separately and then a printed sample of both materials
¹²⁶ to determine if there was possible to observe a chemical bonding. Every sample was measured
¹²⁷ in two different points, three times in each point then curves were normalized and analyzed
¹²⁸ with the Origin Pro 8. The Fourier transform infrared spectra have been recorded in the range
¹²⁹ of 4000 cm^{-1} to 375 cm^{-1} with resolution 4 cm^{-1} using Bruker IFS 66V spectrophotometer.

¹³⁰ **2.2.3 Differential scanning calorimetry –DSC-**

¹³¹ Differential scanning calorimetry analysis were performed with a DSC-1 Mettler Toledo with
¹³² STArE software operating under nitrogen atmosphere at heating rate and cooling rate of
¹³³ $10\text{ }^{\circ}\text{C/min}$. rPET, rHDPE and rPET90//rHDPE10 samples were investigated using three
¹³⁴ cycles: first heating from 20°C to $270\text{ }^{\circ}\text{C}$, cooling to $20\text{ }^{\circ}\text{C}$ and reheating to 270°C . The
¹³⁵ rHDPE sample was analyzed following similar cycles but with the maximum temperature set
¹³⁶ at 250°C and the blend with temperatures from -20 to 270°C . Glass transition temperature
¹³⁷ (T_g) of rPET was determined during the first heating cycle, while rPET90//rHDPE10 (T_g)
¹³⁸ during the second heating cycle along with the melting point of all materials. Crystallization
¹³⁹ temperature (T_c) of the each of the materials was determined during the cooling cycle. The
¹⁴⁰ degree of crystallinity (X_c) was calculated from the second cycle for recycled materials and
¹⁴¹ first cycle for the blend as expressed in equation (1) ([Pan et al., 2020](#); [Taghavi et al., 2018](#)):

$$X_c(\%) = \frac{\Delta H_m}{w \cdot \Delta H_m^{\circ}} \quad (1)$$

¹⁴² Where, ΔH_m is the latent heat of melt, w is weight percentage of polymer in the blend,
¹⁴³ and ΔH_m° is the reference heat of 100% crystalline PET (140 J/g) and HDPE (293 J/g),
¹⁴⁴ respectively, provided in the literature ([Kratofil et al., 2006](#); [Pan et al., 2020](#)).

₁₄₅ **2.2.4 Melt Flow Index –MFI-**

₁₄₆ The melt-flow index (MFI) of rPET90//rHDPE10 flakes was determined using a Instron
₁₄₇ CEAST MF20. The analysis was performed using three samples of ~5 g at 255 °C using
₁₄₈ a 2.16 kg weight according to ASTM D1238. The process was repeated three times. The
₁₄₉ average value of the three results was then reported with *gr/10 × min* unit.

₁₅₀ **2.2.5 Density**

₁₅₁ In order to calculate the material's density, first; the volume was found measuring the dimen-
₁₅₂ sions of a solid 50x50x50 mm cubic geometry fabricated injecting rPET90//rHDPE10 flakes
₁₅₃ into a square mould with a known volume using open-source desktop injection (Holipress,
₁₅₄ Holimaker, France) machine. Then the model was weighed, and the mass was obtained. Fi-
₁₅₅ nally, density was calculated as expressed in Equation 2. To ensure the accuracy the test
₁₅₆ was performed twice and the average value was reported in *g/cm³*.

$$\rho = V/m \quad \left[\frac{g}{cm^3} \right] \quad (2)$$

₁₅₇ Where, ρ is the density, V is the volume, and m the mass.

₁₅₈ Afterwards, experimental results were compared with the theoretical blend density which
₁₅₉ could be calculated by Equation 3.

$$\rho_{12} = \frac{1}{\frac{W_1}{\rho_1} + \frac{W_2}{\rho_2}} \quad \left[\frac{g}{cm^3} \right] \quad (3)$$

₁₆₀ Where, ρ_{12} is the density of the blend, W_1 and W_2 , the weight fractions of each polymer, ρ_1
₁₆₁ and ρ_2 , the theoretical density of each polymer for PET (1.38 *g/cm³*) and HDPE 0.93 to
₁₆₂ 0.97 *g/cm³* ([Jonathan GUIDIGO1 et al., 2017](#)).

₁₆₃ **2.3 Printing process**

₁₆₄ **2.3.1 Establishing optimal parameters**

₁₆₅ Establishing optimum combinations of parameters is essential for better quality and me-
₁₆₆ chanical properties of the printed parts ([Jaisingh Sheoran and Kumar, 2020](#)). According
₁₆₇ to Oberloier et al. ([2022a](#)), particle swarm optimization (PSO) is an effective and time-
₁₆₈ effective method for this purpose. The optimization of the 3-D printing parameters for the
₁₆₉ rPET90//rHDPE10 material in the GigabotX was performed using the open-source PSO Ex-
₁₇₀ perimenter platform (available in Linux), following the methodology developed by Oberloier
₁₇₁ et al. ([2022a](#)). Three process benchmark artifacts were printed; line, plane, and cube. They
₁₇₂ were modeled in CAD software Onshape CAD v1.150 and sliced using Prusaslicer v2.52.0.
₁₇₃ Figure 3 presents the geometry models and dimensions.

Geometry	Lenght (mm)	width (mm)	height (mm)
Line	200	2	1
Plane	100	100	1
Cube	40	40	40

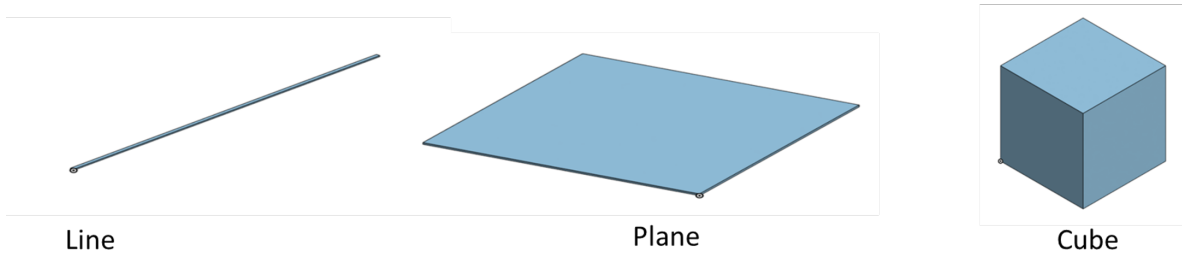


Figure 3: Dimensions and CAD models of the geometries used for parameters optimization.

₁₇₄ Four parameters were assessed: 1) the nozzle temperature, 2) bed temperature, 3) the printing
₁₇₅ speed and 4) extrusion multiplier ([Oberloier et al., 2022b](#)). The initial parameters for the line
₁₇₆ are presented in Table 1a while other parameters were obtained in preliminary experimental
₁₇₇ work shown in Table 1.b. Finally, the PSO tuning parameters were found in the previous
₁₇₈ PSO work ([Oberloier et al., 2022a](#)) Table 1.c.

Table 1: table 1

(a) Line optimization initial parameters

Variable	Min	Max	Guess	True/False	Description
T1	255	270	260	TRUE	Temperature Zone 1 on GigabotX
Tb	80	90	85	TRUE	Bed temperature
Ps	10	25	15	TRUE	Printing Speed
E	0.5	2	1	FALSE	Extrusion Multiplier

(b) Fixed parameters to perform printing parameters optimization based on PSO

Parameters	Value	Units
Layer height	0.5	mm
Width	2	mm
T2	230	°C
T3	220	°C
Cooling	0	%
Infill density	2	%

(c) Recommended parameters for PSO tuning

Variable	Value	Description
Kv	0.5	The emphasis given to the velocity component
Kp	1.0	The emphasis given to a particle's personal best position
Kg	2.0	The emphasis given to the swarm's group best position

2.3.2 Fused Granular Fabrication –FGF-

To print the raw material obtained, a 3-heat-zone modified open-source printer (Gigabot XL re:3D, Houston, TX, USA) was used as illustrated in Figure 4. The machine is a single screw extrusion-based 3-D printer capable of direct printing pellets, flakes or granules, with a nozzle size of 1.75 mm. For this study, a chair was printed to evaluate the ability for the material to 3-D print and the machine capacity to print large-objects such as a piece of furniture. The ideal parameters found for the cube geometry were used to print the final part.

3 Results and discussion

3.1 Material characterization

Both polymeric components of the bottle as well as the blend were characterized and analyzed to determine their properties using different methods as explained in the previous section.

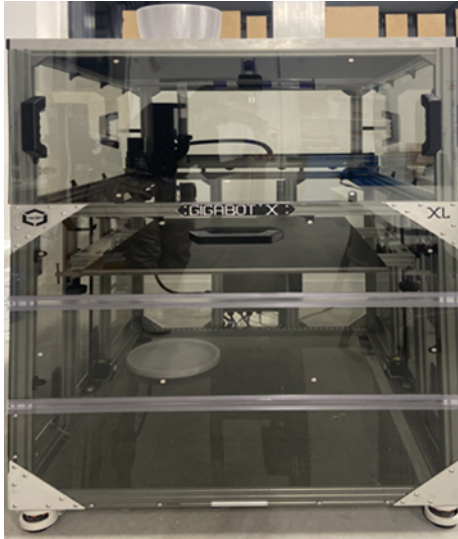


Figure 4: Fused granular fabrication printer Gigabot

190 **3.1.1 Material particle size analysis (granulometry)**

191 The material after shredding has an irregular shape, which led to machine clogging and
192 generated under-extrusion issues, lowering the quality of the prints. Therefore, granulometry
193 evaluation is essential to control these issues. Previous studies demonstrated that particles
194 with areas smaller than 22 mm^2 were optimal for print without jamming or under-extrusion
195 problems (Woern et al., 2018). From the experiments conducted, however, particles with
196 areas above 10 mm^2 clogged in the feeding system and auger screw of the machine. Therefore,
197 granulometry analysis was performed using three different mesh sizes.

198 Figure 5 shows the results obtained, where particles sifted at 5 mm had an average area
199 similar to the reference. There are, however, particles with areas over 9 mm^2 which blocked
200 in the feeding and extrusion section. Particles sifted to 1.5 mm showed a distribution with
201 areas from 0 to proximately 3 mm^2 , this area was considered too low for printing. Small
202 particles can completely melt in the first heat zone obstructing the consistent flow of other
203 particles and not allowing the pressure needed to extrude the melted particles lower in the
204 screw. Although flakes of 3 mm show a more dispersed distribution and slightly lower area
205 compared with the reference, those particles were found to be optimal for printing.

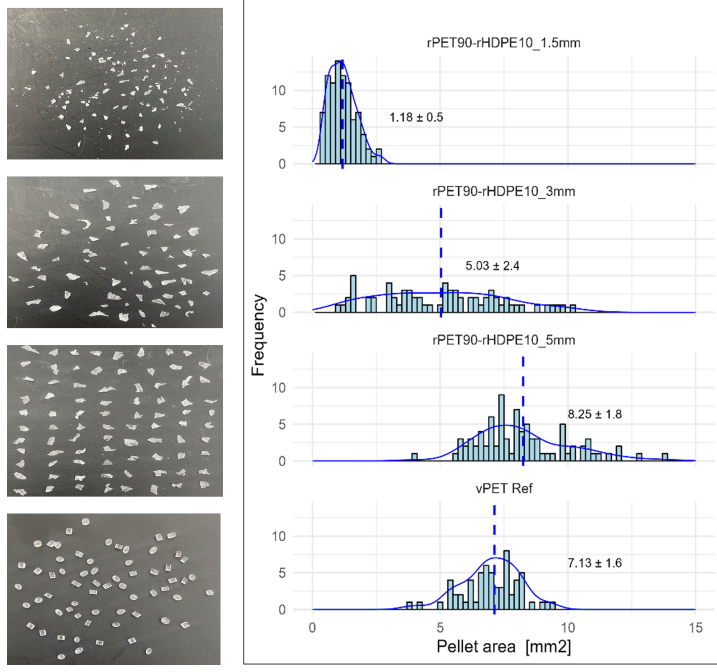


Figure 5: Granulometry analysis

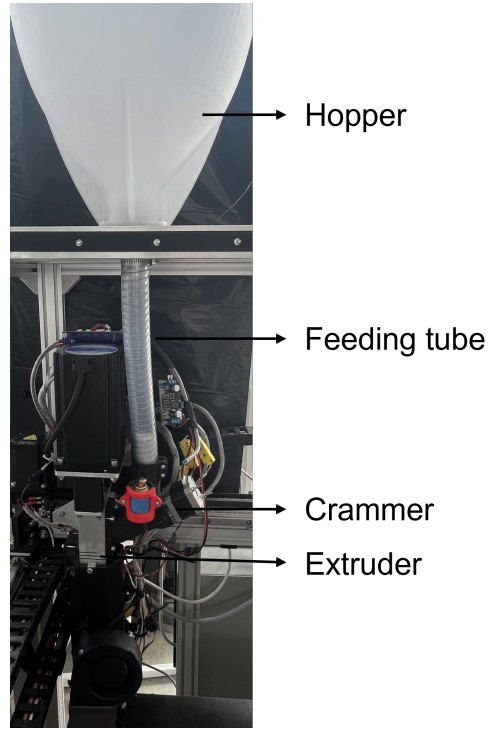


Figure 6: Gigabot feeding system

206 The final objects, however, still displayed under-extrusion issues. For this reason, a crammer
 207 was implemented (Little et al., 2020) as presented in Figure 6; which physically pushes
 208 particles to the auger to convey them from feeding tube into the extruder. After the crammer
 209 implementation under-extrusion issues were significantly decreased. It was concluded that
 210 flakes with areas between 1.5 mm^2 to 10 mm^2 were optimum for print using a crammer able
 211 to aid the feeding system.

212 3.1.2 Chemical analysis from FTIR

213 Chemical structure information of the materials was obtained using FTIR spectroscopy, which
 214 provided analysis of the characteristic spectral bands of the polymers.

215 First, for the rPET (bottle) four characteristic bands can be observed Figure 7, one in
 216 1713cm^{-1} representing the $C = O$ double bond, the $C - O$ single bond ester at 1240cm^{-1} ,
 217 1093cm^{-1} band corresponding to the methylene group and vibrations of the ester bond and
 218 finally, a band 722cm^{-1} the CH₂ rocking bending vibration.

219 Similar results were obtained in the literature for PET coming from recycled water bottles,
 220 soda bottles and food containers (Zander et al., 2018). For rHDPE (caps), four charac-
 221 teristic peaks were observed, the bond of C-H functional group in peaks 2915cm^{-1} and
 222 2847 cm^{-1} , main bending mode of the -CH₂ in 1465 cm^{-1} and CH₂ rocking bending vi-
 223 bration at 729 cm^{-1} . These results confirmed the chemical structures of starting materials.
 224 Additionally, other indicative resonances besides those associated with the polymer structures
 225 were not observed, concluding that additives or plasticizers in significative quantities were
 226 not present in either sample. The spectrum of the printed blend (rPET90//rHDPE10) had
 227 the same characteristic peaks as the bottle, confirming the PET dominant content. There
 228 are, however, observable differences between 1000 cm^{-1} and 720 cm^{-1} and in the bond of C-
 229 H (2915 cm^{-1} and 2847 cm^{-1} peaks), confirming the presence of HDPE (cap). The shifting
 230 observed can be attributed to the hydrogen interactions between both materials.

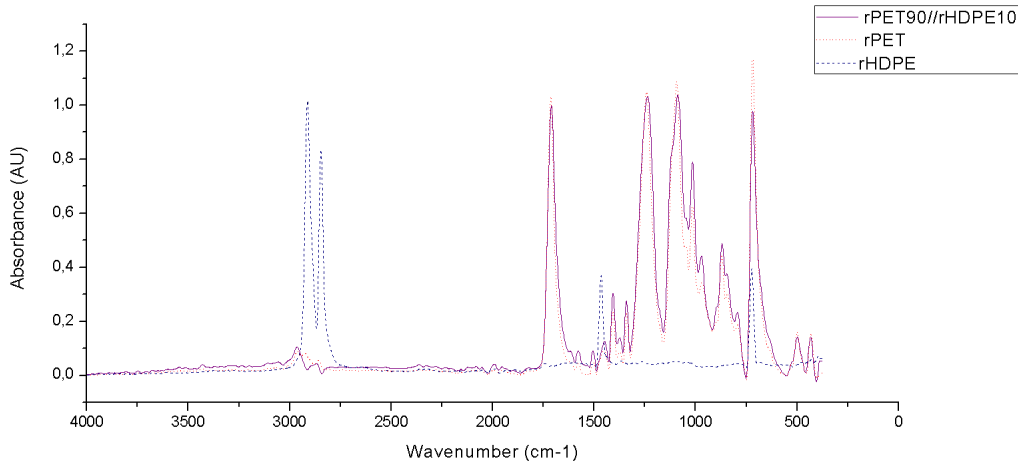


Figure 7: FTIR spectra of rPET, rHDPE and their blend

231 3.1.3 Thermal analysis DSC

232 The thermal properties of both recycled materials and their blend were characterized via
 233 DSC to have a starting point for the 3-D printing process parameter optimization.
 234 From the representative heating and cooling thermograms shown in Fig. 5, two distinct

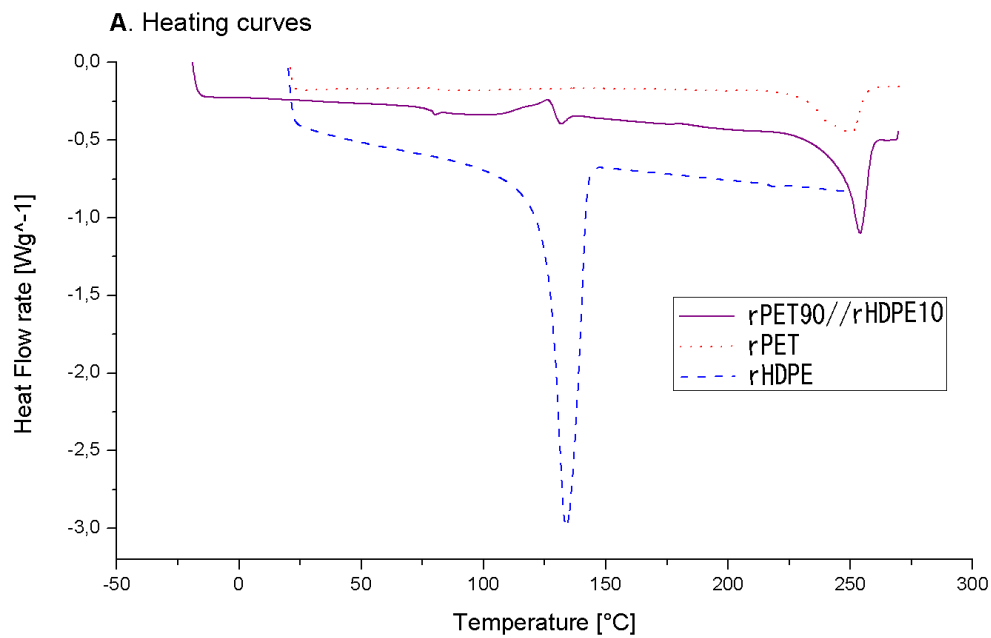
Table 2: Thermal analysis of rPET, rHDPE and their blend

Sample	Glass transition		Melting		Crystallization		% Crystallinity	
	Tg (°C)		Tm (°C)	ΔHm (J/g)	Tc (°C)	ΔHc (J/g)	ΔHcc (J/g)	Xc
rPET	82		249.9	31.6	196.7	34.8	-	22.6
rHDPE	-		133.8	172	118.7	158.5	-	58.7
rPET90/rHDPE10	77 / -		254/131.7	40.3/1.30	210.6/117.4	37.9/6.7	6.8	24.8 / 18.4

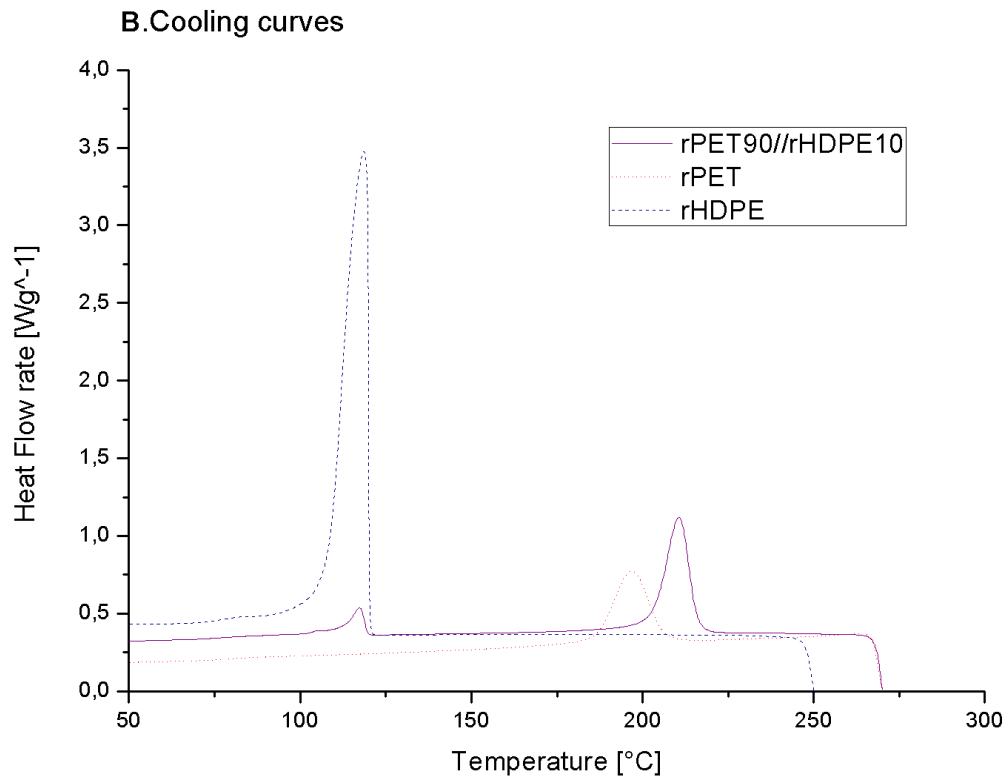
235 endothermic peaks are observed in the printed blend sample that are associated with fusion
 236 of the crystalline fractions of rHDPE and rPET, which confirms the immiscibility of both
 237 materials. Moreover, a significant reduction in the enthalpy of fusion and crystallization of
 238 the rHDPE in the blend is attributed to the low percentage of HDPE in the blend. The
 239 observation of cold crystallization peak in the blend but not in the individual polymers,
 240 however, can be attributed to an interaction between both polymers, where the rHDPE
 241 might act as a nucleating agent. Table 2. list the thermal properties for rPET, rHDPE and
 242 rPET90//rHDPE10. The melting point for rHDPE and rPET are 131.7 °C and 249.9 °C,
 243 respectively and are similar to those found in the literature ([Chen et al., 2015](#); [Lei et al., 2009](#);
 244 [Vaucher et al., 2022](#)). It is observed that the melting and crystallization temperature of rPET
 245 shifted to a higher value, while slightly decreasing for rHDPE. In addition, the crystallization
 246 of rPET was found to be somewhat affected by the addition of rHDPE as it was increased
 247 4%. It is likely the addition of the rHDPE acted as germination point for crystallization
 248 ([Vaucher et al., 2022](#)). The slight changes in the rPET temperatures of fusion-crystallization
 249 and degree of crystallinity showed the interaction of both polymers.

250 3.1.4 Rheology MFI

251 The melt flow index of the flakes was determined, enabling a fast and practical screening of the
 252 viscosity of the material. Following the DSC results, the initial temperature to start the MFI
 253 test was 250°C, however the material did not flow reliably so the temperature was increased by
 254 5°C to enable the melt flow index of the rPET90//rHDPE10 to be determined. A temperature
 255 of 260°C was also tested, however, the material flowed rapidly and the measurement could
 256 not be reliably obtained. MFI tests were performed three times and the results of the



(a) Heating curves



(b) Cooling curve

Figure 8: DSC thermograms of recycled materials and blends

257 rPET90//rHDPE10 was a medium MFI 39.4 ± 2.4 g/10min, which is roughly consistent
258 with values found in literature for rPET ([Bustos Seibert et al., 2022](#); [Langer et al., 2020](#);
259 [Nofar and Oğuz, 2019](#)). This result suggests that the low percentage addition of HDPE do
260 not highly impact the MFI value of rPET. As the material flowed at temperature of 255°C
261 in the MFI, it provided the input temperature for 3-D printer parameters optimization.

262 3.1.5 Density

263 The density allows the estimation of cost, material use, time consumed and weight of the
264 printing object in the slicer. This information is useful to find the accurate printing param-
265 eters with the PSO experimenter as fitness is calculated as a function of the dimensional
266 accuracy and weight of the printed object. Hence, density was useful to determine the weight
267 of the geometries.

268 From calculations made after weight and measuring the rPET90//rHDPE10 injected object,
269 the density of the material was found to be 1.13 g/cm^3 . The inclusion of HDPE in the
270 matrix polymer led to a slight decrease in its density, which is a common outcome when a
271 polymer is mixed with a lower density polymer. However, if we consider a PET/HDPE blend
272 with a mass ratio of 90/10, the calculated theoretical density is 1.32 g/cm^3 . The observed
273 decrease of 14% in the results could be attributed to factors such as experimental conditions
274 and manual measurements

275 3.2 Particle swarm optimization (PSO) Experimenter

276 Geometries were 3-D printed changing the parameters as expressed in the PSO Experimenter
277 software. The fitness function is defined by the weighted sum of the dimensional measure-
278 ments (length, width, height, and weight) of the printed object, where fitness below 0.1 was
279 set as a desirable threshold. In the software five particles were established for one iteration,
280 thus in one iteration five different parameters combinations were printed. The first geometry
281 (line) was able to reach a fitness of < 0.1 after six iterations for a total of thirty lines printed.
282 The ideal parameters for this geometry are listed in column two of Table [Table 3](#) and images

283 of the resulting geometries are illustrated in Figure 9 .

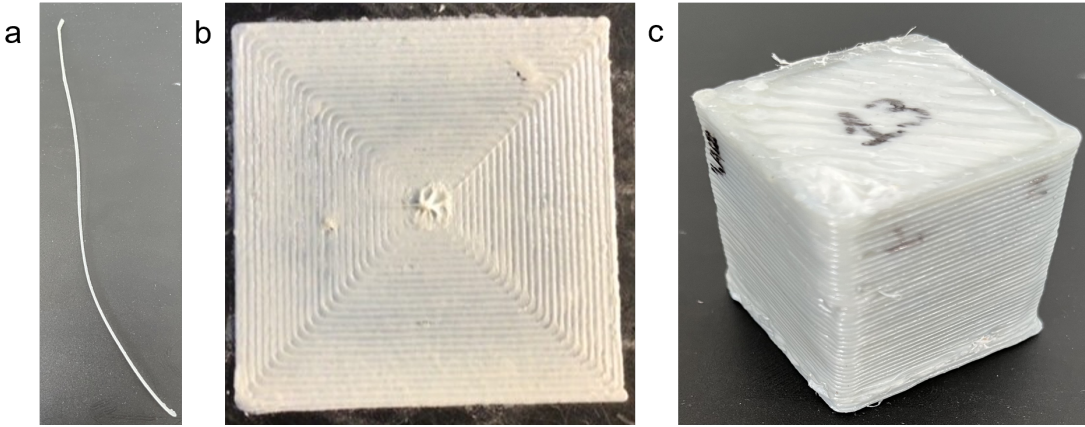


Figure 9: Images of the resulting geometries a) line, b) plane, c) cube

284 Afterwards, these parameters were used as initial guess for plane geometry, which reached
285 the desired fitness in the first iteration. Likewise, cubes were printed using the plane ideal
286 parameter as initial guess and optimal parameters, where found in the first iteration. Results
287 showed a significant change in the printing speed, which lowers at higher geometry complexity.
288 Moreover, the cube geometry required a higher extrusion multiplier to fill gaps and overcome
289 under-extrusion problems. The optimization of the parameters for the three geometries took
290 around 10h reducing the experimental time, compared with conventional methods. According
291 to Oberloier et al. (2022a) this time of experimentation can be reduced 97%. Indeed, the
292 efficacy of PSO in finding global optimum parameters is high, particularly when there is a
293 large or complex design space (Saad et al., 2019; Selvam et al., 2020).

294 Additionally, PSO converge to optimum solutions with fewer iterations than DoE methods
295 (Zhang et al., 2015) while mixing PSO with other meta-heuristic methods has shown higher
296 ability of predict and optimize parameters (e.g. minimize surface roughness(Shirmohammadi
297 et al., 2021), compressive strength and porosity of scaffolds (Asadi-Eydivand et al., 2016),
298 mechanical properties(Raju et al., 2019)). However, the DoE methods are still widely used
299 as they provide insight into the effects of individual design parameters and their interactions
300 while the ability to find interaction between the variables is not possible using PSO. In the
301 beginning of a set of optimization experiments, the complete understanding of the process

302 technique as well as the function settings might be complex. The methodology used in this
303 study, however, was easy to implement and the software has the advantage of being free, open
304 source and user-friendly, lessening the initial difficulty. Thus, PSO demonstrated to be an
305 effective and high accuracy prediction technique able to find the initial optimum parameters
306 for rPET90//rHDPE10 material for FGF/FPF.

307 From the results it is observe that the optimal parameters may change depending of the object
308 printed and each parameter has its own variation. One hypothesis is that geometry might
309 play a role in parameter assignment and probably could be more visible in larger prints, yet
310 this hypothesis needs further investigation. There are several physical mechanisms at play
311 that would be expected to change optimal printing parameters based on the geometry and
312 size of the object. For example, the cooling time and temperature history of a voxel will
313 depend on the geometry of the printed object. Thus, to maintain the same thermal history
314 the printing parameters must change as the geometry changes. This same effect of thermal
315 history can also have more subtle impacts such as degree of crystallization even for PLA
316 ([Wijnen et al., 2018](#)).

317 In addition, some physical effects of materials extrusion are magnified with scale. The most
318 obvious is the impacts of thermal expansion and contraction. Small changes in contraction
319 as a part cools may cause acceptable distortions for small prints, but these are magnified
320 for large prints (e.g. causing deformation and in the worst cases delamination or loss of bed
321 adhesion)([Shah et al., 2019](#)). Although, Roschli et al. ([2019](#)) showed the obstacles and
322 possible solutions of the large-scale AM according to the way of the parts are designed the
323 incidence of the geometry in the printing parameters needs far more detailed future studies.
324 Specifically better models for mapping 3-D printing parameter optimizations of small printed
325 objects to large volume objects is needed.

326 Table 3. Ideal printing parameters for fused granule fabrication of waste PET and HDPE
327 blend made from shredded whole plastic water bottles.

Table 3: Ideal printing parameters for fused granule fabrication of waste PET and HDPE blend made from shredded whole plastic water bottles

Variable	Line value	Planes value	Cube value	Δ	Units
T1	258	263	264	6 \pm 3.2	°C
Tb	86	82	84	4 \pm 2	°C
Ps	21	14	10	11 \pm 5.6	mm/s
E	1.07	0.87	1.32	0.5 \pm 0.3	-

328 3.3 Functional object print

329 The ideal parameters found for the cube geometry were used as final parameters for print the
 330 case study product, except the print speed for the optimized line speed was used to decrease
 331 the printing time and delamination. This change was performed as according to the PSO
 332 results the material is printable in a range of 10 to 20 mm/s. Additionally, the faster the
 333 printing the lesser the time of cooling between the layers thus avoiding possible delamination
 334 ([Roschli et al., 2019](#)), which is exacerbated for larger objects.

335 The Gigabot X successfully produced a piece of furniture from multi-material recycled water
 336 bottles that included mixing HDPE and PET as shown in Fig. 6.a.

337 The printing quality is acceptable as a prototype, proven the machine capacity of printing
 338 large-scale functional objects where the chair was able to hold a child with a mass of 20 kg
 339 comfortably as shown in Fig.6 f. The material, in the other hand, needs further evaluation
 340 as the printed object showed weak bond strength between the adjacent layers (delamination
 341 Fig. 6.b).This is probably due to the difference in chemical properties of both materials or
 342 immiscibility [William et al. \(2021\)](#), high crystallinity ([Verma et al., 2023](#)) and the large
 343 volume of the object as delamination issues were more visible at the time of print the chair
 344 that in the parameters optimization process. Indeed, delamination presented in the printing
 345 of a larger object can be attributed to the rapid cooling of the layers before the material
 346 is once again deposited contrary of the cube printing where the small surface allowing the
 347 adhesion of layers before there are completely cooled. This can even be an issue for more
 348 popular 3-D printing materials like PLA from the print surface ([Wijnen et al., 2018](#)). The

addition of agents that reduce the interphase tension between polymers might help to solve the delamination present and enhance the properties of the material (Dai et al., 1997; Inoya et al., 2012; Kramer et al., 1994) as interfacial bond can be enhanced by polymer modification (Gao et al., 2021) and viscosity decrement (Ko et al., 2019). Additionally, while printing warping problems were observed, (Fig. 6.c) which are likely caused by the high crystallization rates of HDPE (Schirmeister et al., 2019) suggesting that the incorporation of this plastic even in a low portions have affected the printing negatively. The use of Magigoo adhesive (Thought3D Ltd., Paola, Malta) and the addition of a brim was tested in order to enable bed adhesion, yet this solutions did not completely solve the problem. A previous study showed that the use of a building plate made of thermoplastic elastomer SEBS allowed the adhesion of the plastic and enables facile detachments of the printing object without breaking or damaging (Schirmeister et al., 2019), suggesting a solution that needs further evaluation in future work. Another visible issue present in the close angles of the printed object was the shrinkage (Fig. 6.d) which occurs during solidification and especially upon polymer crystallization. Moreover, as is well-know, PET has hygroscopic tendencies and easily absorbs atmosphere moisture making it difficult to extrude (Bustos Seibert et al., 2022) thus is likely to break down in the presence of water, lowering the quality of the print. Before the chair printing some samples showed brittle behavior and voids formation therefore, the material was constantly dried and the hopper was closed in order to avoid moisture coming from the environment helping to have a more printable material. Visually it can be observed some vibration and ringing problems (Fig. 6.e) caused by the machine upgrading, both acceleration and jerk (maximum value of the instantaneous speed change) needs finer tuning.

3.3.1 Cost and environmental impact

The printing time took 10 h and the printed object has a mass of 840 g. Due to the found optimized speed being low, the printing rate (grams per hour) is low considering the machine that pellet printers have a typical throughput of 220 g to 9 kg per hour. The printing time could be improved by upgrading the extruder motor to a more powerful one. Besides, the

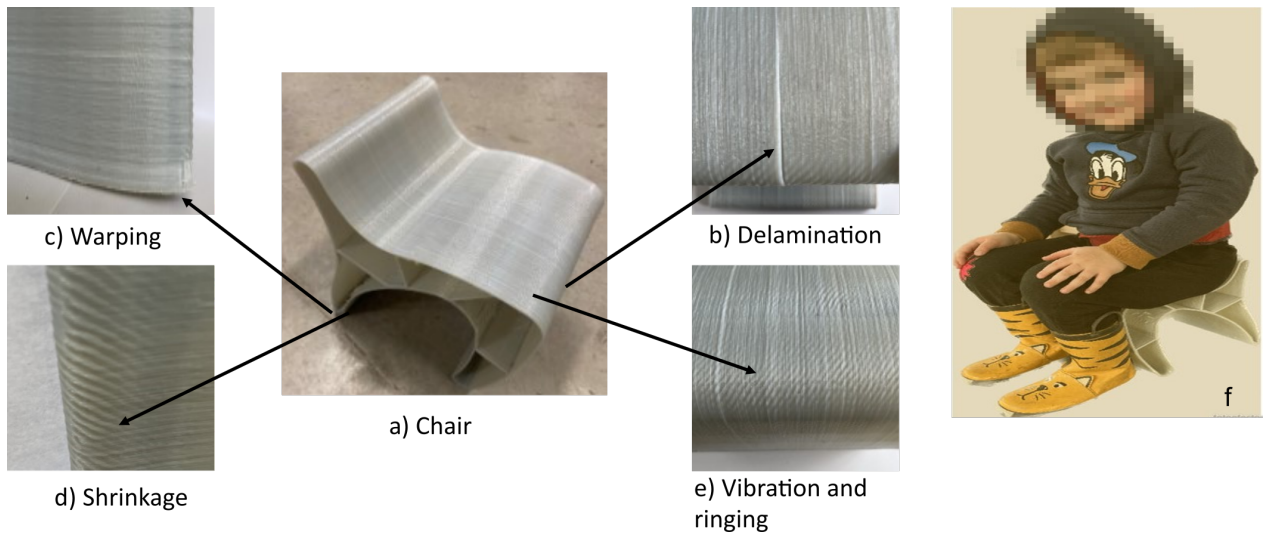


Figure 10: Finished children chair and printing issues

³⁷⁶ energy required for 10 hr of 3-D printing was found to be 6 kW-hr resulting in a production
³⁷⁷ cost of ~1.2 € in function of the electricity cost in France, without considering the material
³⁷⁸ cost as bottles were obtained from post-consumers waste. When labor costs are not included
³⁷⁹ the price was significative reduced (~88%) compared with those low cost found in the market.

³⁸⁰ The economics of fabricating the case study product remained competitive even if recycled
³⁸¹ plastic pellets or shreds are used, which can be found on the market from 1-10 €/kg. However,
³⁸² labor, maintenance and machine devaluation were not considered in the final price and are
³⁸³ needed in future work for a complete economic evaluation.

³⁸⁴ Regarding the environmental impact, although this study does not evaluate the entire life
³⁸⁵ cycle of the printed object, various scientific studies have already shown feasibility of dis-
³⁸⁶ tributed recycling ([Kerdlap et al., 2022](#); [Santander et al., 2020](#)), the comparation between
³⁸⁷ conventional and distributed manufacturing in terms of energy consumption and emissions
³⁸⁸ ([Kreiger and Pearce, 2013](#)), environmental performance of AM [Colorado et al. \(2020\)](#) and
³⁸⁹ the appearance of DRAM as a source of raw material for diverse 3-D printers coming from
³⁹⁰ post-consumer plastic waste in the form of either filament ([Hart et al., 2018](#); [Mikula et al.,](#)
³⁹¹ [2021](#); [Mohammed et al., 2017b](#); [Pakkanen et al., 2017b](#)) or granules ([Alexandre et al., 2020](#)).

392 Additionally, Caceres-Mendoza et al. (2023) has developed a complete life of cycle assess-
393 ment of a DRAM system based on the production of PLA filament comparing virgin and
394 recycled materials. Their environmental results showed a reduction of the impacts of produc-
395 tion (climate change, fossil depletion, water depletion and potential eutrophication) of ~97%
396 compared to virgin filament. These results, however, are dependent on the energy supply
397 and can vary depending on location.

398 4 Conclusion and future work

399 This study analyzed the feasibility of using mixed post-consumer waste as feedstock material
400 for direct 3-D printing without compatibilization. The results showed the potential of mixing
401 solid waste plastics (PET/HDPE) for its use as feedstock material by printing a water bottle
402 with two incompatible polymers from the cap and body of the bottle. Additionally, the results
403 showed that a large-scale FGF 3-D printer was capable of producing a cost-effective functional
404 object from these mixed waste PET/HDPE plastics. Further research is needed in the analysis
405 of mechanical properties of the material as well as the possibilities of using compatibilizers
406 capable of enhancing the interphase tension between plastics and lower their crystallinity,
407 which might help improve performance and enhance material and 3-D printed part properties.
408 These factors increase in importance as the scale of the 3-D printed part increases. The
409 improvement of the material science of the approach can also offer an opportunity to improve
410 the quality of the printing printing time, lowering the energy consumption of the machine
411 and thus improving the economic viability of DRAM with mixed plastic waste.

412 In addition, future work could assess the different types of combinations or blends between
413 commodity plastics using or not compatibilizer towards its printability, bringing out the
414 possibility of selection/sorting process elimination. In the same way, the development of
415 a methodology that allows the reproducibility of the process even in areas with limited
416 infrastructure opens up the potential of plastic revalorization using DRAM.

⁴¹⁷ **Declaration of competing**

⁴¹⁸ The authors declare that they have no known competing financial interest or personal rela-
⁴¹⁹ tionships that could have appeared to influence the work reported in this paper. Acknowl-
⁴²⁰ edgements

⁴²¹ **Acknowledgements**

⁴²² This project has received funding from the European Union's Horizon 2020 research and
⁴²³ innovation programme under the grant agreement No 869952. The authors thank the LUE
⁴²⁴ program for the financing of the thesis, the Lorraine Fab Living lab platform and the Thomp-
⁴²⁵ son endowment.

426 **References**

- 427 Alexandre, A., Cruz Sanchez, F.A., Boudaoud, H., Camargo, M., Pearce, J.M., 2020. Me-
428 chanical Properties of Direct Waste Printing of Polylactic Acid with Universal Pellets
429 Extruder: Comparison to Fused Filament Fabrication on Open-Source Desktop Three-
430 Dimensional Printers. *3D Printing and Additive Manufacturing* 7, 237–247. <https://doi.org/10.1089/3dp.2019.0195>
- 432 Anderson, I., 2017. Mechanical Properties of Specimens 3D Printed with Virgin and Recycled
433 Polylactic Acid. *3D Printing and Additive Manufacturing* 4, 110–115. <https://doi.org/10.1089/3dp.2016.0054>
- 435 Asadi-Eydivand, M., Solati-Hashjin, M., Fathi, A., Padashi, M., Abu Osman, N.A., 2016.
436 Optimal design of a 3D-printed scaffold using intelligent evolutionary algorithms. *Applied
437 Soft Computing* 39, 36–47. <https://doi.org/10.1016/j.asoc.2015.11.011>
- 438 Attaran, M., 2020. 3D Printing Role in Filling the Critical Gap in the Medical Supply Chain
439 during COVID-19 Pandemic. *American Journal of Industrial and Business Management*
440 10, 988–1001. <https://doi.org/10.4236/ajibm.2020.105066>
- 441 Baechler, C., DeVuono, M., Pearce, J.M., 2013. Distributed recycling of waste polymer into
442 RepRap feedstock. *Rapid Prototyping Journal* 19, 118–125. <https://doi.org/10.1108/13552541311302978>
- 444 Bowyer, A., 2014. 3D Printing and Humanity's First Imperfect Replicator. *3D Printing and
445 Additive Manufacturing* 1, 4–5. <https://doi.org/10.1089/3dp.2013.0003>
- 446 Bustos Seibert, M., Mazzei Capote, G.A., Gruber, M., Volk, W., Osswald, T.A., 2022. Man-
447 ufacturing of a PET Filament from Recycled Material for Material Extrusion (MEX).
448 *Recycling* 7, 69. <https://doi.org/10.3390/recycling7050069>
- 449 Byard, D.J., Woern, A.L., Oakley, R.B., Fiedler, M.J., Snabes, S.L., Pearce, J.M., 2019.
450 Green fab lab applications of large-area waste polymer-based additive manufacturing.
451 *Additive Manufacturing* 27, 515–525. <https://doi.org/10.1016/j.addma.2019.03.006>
- 452 Caceres-Mendoza, C., Santander-Tapia, P., Cruz Sanchez, F.A., Troussier, N., Camargo,
453 M., Boudaoud, H., 2023. Life cycle assessment of filament production in distributed
454 plastic recycling via additive manufacturing. *Cleaner Waste Systems* 5, 100100. <https://doi.org/10.1016/j.clwas.2023.100100>
- 456 Carrete, I.A., Quiñonez, P.A., Bermudez, D., Roberson, D.A., 2021. Incorporating Textile-
457 Derived Cellulose Fibers for the Strengthening of Recycled Polyethylene Terephthalate
458 for 3D Printing Feedstock Materials. *Journal of polymers and the environment*.
- 459 Chen, R.S., Ab Ghani, M.H., Salleh, M.N., Ahmad, S., Tarawneh, M.A., 2015. Mechanical,
460 water absorption, and morphology of recycled polymer blend rice husk flour biocomposites.
461 *Journal of Applied Polymer Science* 132. <https://doi.org/10.1002/app.41494>
- 462 Chong, S., Pan, G.-T., Khalid, M., Yang, T.C.-K., Hung, S.-T., Huang, C.-M., 2017. Phys-
463 ical Characterization and Pre-assessment of Recycled High-Density Polyethylene as 3D

- 464 Printing Material. *Journal of Polymers and the Environment* 25, 136–145. <https://doi.org/10.1007/s10924-016-0793-4>
- 465
- 466 Choong, Y.Y.C., Tan, H.W., Patel, D.C., Choong, W.T.N., Chen, C.-H., Low, H.Y., Tan, M.J., Patel, C.D., Chua, C.K., 2020. The global rise of 3D printing during the COVID-19 pandemic. *Nat Rev Mater* 5, 637–639. <https://doi.org/10.1038/s41578-020-00234-3>
- 467
- 468
- 469 Chu, J.S., Koay, S.C., Chan, M.Y., Choo, H.L., Ong, T.K., 2022. Recycled plastic filament made from post-consumer expanded polystyrene and polypropylene for fused filament fabrication. *Polymer Engineering & Science* 62, 3786–3795. <https://doi.org/10.1002/pen.26144>
- 470
- 471
- 472
- 473 Colorado, H.A., Velásquez, E.I.G., Monteiro, S.N., 2020. Sustainability of additive manufacturing: The circular economy of materials and environmental perspectives. *Journal of Materials Research and Technology* 9, 8221–8234. <https://doi.org/10.1016/j.jmrt.2020.04.062>
- 474
- 475
- 476
- 477 Corsini, L., Aranda-Jan, C.B., Moultrie, J., 2022. The impact of 3D printing on the humanitarian supply chain. <https://doi.org/10.17863/CAM.51226>
- 478
- 479 Cruz Sanchez, F.A., Boudaoud, H., Camargo, M., Pearce, J.M., 2020. Plastic recycling in additive manufacturing: A systematic literature review and opportunities for the circular economy. *Journal of Cleaner Production* 264, 121602. <https://doi.org/10.1016/j.jclepro.2020.121602>
- 480
- 481
- 482
- 483 Cruz Sanchez, F.A., Boudaoud, H., Hoppe, S., Camargo, M., 2017. Polymer recycling in an open-source additive manufacturing context: Mechanical issues. *Additive Manufacturing* 17, 87–105. <https://doi.org/10.1016/j.addma.2017.05.013>
- 484
- 485
- 486 Dai, C.-A., Jandt, K.D., Iyengar, D.R., Slack, N.L., Dai, K.H., Davidson, W.B., Kramer, E.J., Hui, C.-Y., 1997. Strengthening Polymer Interfaces with Triblock Copolymers. *Macromolecules* 30, 549–560. <https://doi.org/10.1021/ma960396s>
- 487
- 488
- 489 Dertinger, S.C., Gallup, N., Tanikella, N.G., Grasso, M., Vahid, S., Foot, P.J.S., Pearce, J.M., 2020. Technical pathways for distributed recycling of polymer composites for distributed manufacturing: Windshield wiper blades. *Resources, Conservation and Recycling* 157, 104810. <https://doi.org/10.1016/j.resconrec.2020.104810>
- 490
- 491
- 492
- 493 Despeisse, M., Baumers, M., Brown, P., Charnley, F., Ford, S.J., Garmulewicz, A., Knowles, S., Minshall, T.H.W., Mortara, L., Reed-Tsochas, F.P., Rowley, J., 2017. Unlocking value for a circular economy through 3D printing: A research agenda. *Technological Forecasting and Social Change* 115, 75–84. <https://doi.org/10.1016/j.techfore.2016.09.021>
- 494
- 495
- 496
- 497 Evode, N., Qamar, S.A., Bilal, M., Barceló, D., Iqbal, H.M.N., 2021. Plastic waste and its management strategies for environmental sustainability. *Case Studies in Chemical and Environmental Engineering* 4, 100142. <https://doi.org/10.1016/j.cscee.2021.100142>
- 498
- 499
- 500 Fontana, L., Giubilini, A., Arrigo, R., Malucelli, G., Minetola, P., 2022. Characterization of 3D Printed Polylactic Acid by Fused Granular Fabrication through Printing Accuracy, Porosity, Thermal and Mechanical Analyses. *Polymers* 14, 3530. <https://doi.org/10.1016/j.cscee.2021.100142>
- 501
- 502

- 503 3390/polym14173530
- 504 Ford, S., Despesse, M., 2016. Additive manufacturing and sustainability: An exploratory
505 study of the advantages and challenges. Journal of Cleaner Production 137, 1573–1587.
506 <https://doi.org/10.1016/j.jclepro.2016.04.150>
- 507 Gaikwad, V., Ghose, A., Cholake, S., Rawal, A., Iwato, M., Sahajwalla, V., 2018. Trans-
508 formation of E-Waste Plastics into Sustainable Filaments for 3D Printing. ACS Sustainable
509 Chemistry & Engineering 6, 14432–14440. <https://doi.org/10.1021/acssuschemeng.8b03105>
- 510 Gallup, N., Bow, J.K., Pearce, J.M., 2018. Economic Potential for Distributed Manufacturing
511 of Adaptive Aids for Arthritis Patients in the U.S. Geriatrics 3, 89. <https://doi.org/10.3390/geriatrics3040089>
- 512 Gao, X., Qi, S., Kuang, X., Su, Y., Li, J., Wang, D., 2021. Fused filament fabrication
513 of polymer materials: A review of interlayer bond. Additive Manufacturing 37, 101658.
514 <https://doi.org/10.1016/j.addma.2020.101658>
- 515 Garcia, F.L., Moris, V.A. da S., Nunes, A.O., Silva, D.A.L., 2018. Environmental perfor-
516 mance of additive manufacturing process – an overview. Rapid Prototyping Journal 24,
517 1166–1177. <https://doi.org/10.1108/RPJ-05-2017-0108>
- 518 Geyer, R., 2020. Chapter 2 - Production, use, and fate of synthetic polymers, in: Letcher,
519 T.M. (Ed.), Plastic Waste and Recycling. Academic Press, pp. 13–32. <https://doi.org/10.1016/B978-0-12-817880-5.00002-5>
- 520 Geyer, R., Jambeck, J.R., Law, K.L., 2017. Production, use, and fate of all plastics ever
521 made. Science Advances 3, e1700782. <https://doi.org/10.1126/sciadv.1700782>
- 522 Grassi, G., Spagnolo, S.L., Paoletti, I., 2019. Fabrication and durability testing of a 3D
523 printed façade for desert climates. Additive Manufacturing 28, 439.
- 524 Gwamuri, J., Franco, D., Khan, K.Y., Gauchia, L., Pearce, J.M., 2016. High-Efficiency Solar-
525 Powered 3-D Printers for Sustainable Development. Machines 4, 3. <https://doi.org/10.3390/machines4010003>
- 526 Hart, K.R., Frketic, J.B., Brown, J.R., 2018. Recycling meal-ready-to-eat (MRE) pouches
527 into polymer filament for material extrusion additive manufacturing. Additive Manufac-
528 turing 21, 536–543. <https://doi.org/10.1016/j.addma.2018.04.011>
- 529 ImageJ, 2023. Image processing and analysis in java [WWW Document]. URL <https://imagej.nih.gov/ij/download.html> (accessed 6.13.2023).
- 530 Inoya, H., Wei Leong, Y., Klinklai, W., Thumsorn, S., Makata, Y., Hamada, H., 2012. Compatibilization of recycled poly (ethylene terephthalate) and polypropylene blends:
531 Effect of polypropylene molecular weight on homogeneity and compatibility. Journal of
532 applied polymer science 124, 3947–3955.
- 533 Jaisingh Sheoran, A., Kumar, H., 2020. Fused Deposition modeling process parameters opti-
534 mization and effect on mechanical properties and part quality: Review and reflection on
535 present research. Materials Today: Proceedings, International Conference on Mechanical

- 542 and Energy Technologies 21, 1659–1672. <https://doi.org/10.1016/j.matpr.2019.11.296>
- 543 Jonathan GUIDIGO¹, Stéphane MOLINA², Edmond C. ADJOVI³, André MERLIN
544 4, DONNOT André⁵, Merlin SIMO TAGNE⁶, 2017. Polyethylene Low and High
545 Density-Polyethylene Terephthalate and Polypropylene Blend as Matrices for Wood
546 Flour, in: International Journal of Science and Research (IJSR). pp. 1069–1074.
547 <https://doi.org/10.21275/ART20164296>
- 548 Jones, R., Haufe, P., Sells, E., Iravani, P., Olliver, V., Palmer, C., Bowyer, A., 2011.
549 RepRap – the replicating rapid prototyper. Robotica 29, 177–191. <https://doi.org/10.1017/S026357471000069X>
- 550 Kerdlap, P., Purnama, A.R., Low, J.S.C., Tan, D.Z.L., Barlow, C.Y., Ramakrishna, S.,
551 2022. Comparing the environmental performance of distributed versus centralized plastic
552 recycling systems: Applying hybrid simulation modeling to life cycle assessment. Journal
553 of Industrial Ecology 26, 252–271. <https://doi.org/10.1111/jiec.13151>
- 554 King, D., Babasola, A., Rozario, J., Pearce, J., 2014. Mobile Open-Source Solar-Powered
555 3-D Printers for Distributed Manufacturing in Off-Grid Communities. Challenges in
556 Sustainability 2. <https://doi.org/10.12924/cis2014.02010018>
- 557 Ko, Y.S., Herrmann, D., Tolar, O., Elspass, W.J., Brändli, C., 2019. Improving the filament
558 weld-strength of fused filament fabrication products through improved interdiffusion. Additive
559 Manufacturing 29, 100815. <https://doi.org/10.1016/j.addma.2019.100815>
- 560 Kramer, E.J., Norton, L.J., Dai, C.-A., Sha, Y., Hui, C.-Y., 1994. Strengthening polymer
561 interfaces. Faraday Discussions 98, 31–46. <https://doi.org/10.1039/FD9949800031>
- 562 Kratofil, L., Hrnjak-Murgić, Z., Jelencć, J., Andrićć, B., Kovacé, T., Merzel, V., 2006. Study
563 of the compatibilizer effect on blends prepared from waste poly (ethylene-terephthalate)
564 and high density polyethylene. International Polymer Processing 21, 328–335.
- 565 Kreiger, M.a., Mulder, M.L., Glover, A.G., Pearce, J.M., 2014. Life cycle analysis of dis-
566 tributed recycling of post-consumer high density polyethylene for 3-D printing filament.
567 Journal of Cleaner Production 70, 90–96. <https://doi.org/10.1016/j.jclepro.2014.02.009>
- 568 Kreiger, M.A., Mulder, M.L., Glover, A.G., Pearce, J.M., 2014. Life cycle analysis of dis-
569 tributed recycling of post-consumer high density polyethylene for 3-D printing filament.
570 Journal of Cleaner Production 70, 90–96. <https://doi.org/10.1016/j.jclepro.2014.02.009>
- 571 Kreiger, M., Pearce, J.M., 2013. Environmental Impacts of Distributed Manufacturing from
572 3-D Printing of Polymer Components and Products. MRS Proceedings 1492, 85–90.
573 <https://doi.org/10.1557/opl.2013.319>
- 574 Langer, E., Bortel, K., Waskiewicz, S., Lenartowicz-Klik, M., 2020. Methods of PET Re-
575 cycling, Plasticizers Derived from Post-Consumer PET. [https://doi.org/10.1016/b978-0-323-46200-6.00005-2](https://doi.org/10.1016/b978-0-
576 323-46200-6.00005-2)
- 577 Lei, Y., Wu, Q., Zhang, Q., 2009. Morphology and properties of microfibrillar composites
578 based on recycled poly (ethylene terephthalate) and high density polyethylene. Compos-
579 ites Part A: Applied Science and Manufacturing 40, 904–912. <https://doi.org/10.1016/j.j.>

- 581 **compositesa.2009.04.017**
- 582 Lipsky, S., Przyjemska, A., Velasquez, M., Gershenson, J., 2019. 3D Printing for Human-
583 itarian Relief: The Printer Problem, in: 2019 IEEE Global Humanitarian Technology
584 Conference (GHTC). pp. 1–7. <https://doi.org/10.1109/GHTC46095.2019.9033053>
- 585 Little, H.A., Tanikella, N.G., J. Reich, M., Fiedler, M.J., Snabes, S.L., Pearce, J.M., 2020.
586 Towards Distributed Recycling with Additive Manufacturing of PET Flake Feedstocks.
587 Materials 13, 4273. <https://doi.org/10.3390/ma13194273>
- 588 Löschke, S.K., Mai, J., Proust, G., Brambilla, A., 2019. Microtimber: The Development of
589 a 3D Printed Composite Panel Made from Waste Wood and Recycled Plastics. Digital
590 Wood Design 24, 827–848. https://doi.org/10.1007/978-3-030-03676-8_33
- 591 MacArthur, E., 2017. Beyond plastic waste. Science 358, 843–843. <https://doi.org/10.1126/science.aao6749>
- 592 Mikula, K., Skrzypczak, D., Izydorczyk, G., Warchoł, J., Moustakas, K., Chojnacka, K.,
593 Witek-Krowiak, A., 2021. 3D printing filament as a second life of waste plastics—a
594 review. Environmental Science and Pollution Research 28, 12321–12333. <https://doi.org/10.1007/s11356-020-10657-8>
- 595 Mohammed, M.I., Das, A., Gomez-Kervin, E., Wilson, D., Gibson, I., 2017a. EcoPrinting:
596 Investigating the Use of 100% Recycled Acrylonitrile Butadiene Styrene (ABS) for
597 Additive Manufacturing. University of Texas at Austin.
- 598 Mohammed, M.I., Mohan, M., Das, A., Johnson, M.D., Badwal, P.S., McLean, D., Gibson, I.,
599 2017b. A low carbon footprint approach to the reconstitution of plastics into 3D-printer
600 filament for enhanced waste reduction. KnE Engineering 234–241. <https://doi.org/10.18502/keg.v2i2.621>
- 601 Mohammed, M.I., Wilson, D., Gomez-Kervin, E., Rosson, L., Long, J., 2018. EcoPrinting:
602 Investigation of Solar Powered Plastic Recycling and Additive Manufacturing for En-
603 hanced Waste Management and Sustainable Manufacturing, in: 2018 IEEE Conference
604 on Technologies for Sustainability (SusTech). IEEE, pp. 1–6. <https://doi.org/10.1109/SusTech.2018.8671370>
- 605 Nofar, M., Oğuz, H., 2019. Development of PBT/Recycled-PET Blends and the Influence
606 of Using Chain Extender. Journal of Polymers and the Environment 27, 1404–1417.
607 <https://doi.org/10.1007/s10924-019-01435-w>
- 608 Novak, J.I., Loy, J., 2020. A critical review of initial 3D printed products responding to
609 COVID-19 health and supply chain challenges. Emerald Open Research 2, 24. <https://doi.org/10.35241/emeraldopenres.13697.1>
- 610 Oberloier, S., Whisman, N.G., Pearce, J.M., 2022a. Finding Ideal Parameters for Recycled
611 Material Fused Particle Fabrication-Based 3D Printing Using an Open Source Software
612 Implementation of Particle Swarm Optimization. 3D Printing and Additive Manufactur-
613 ing. <https://doi.org/10.1089/3dp.2022.0012>
- 614 Oberloier, S., Whisman, N.G., Pearce, J.M., 2022b. Finding Ideal Parameters for Recycled

- 620 Material Fused Particle Fabrication-Based 3D Printing Using an Open Source Software
621 Implementation of Particle Swarm Optimization. 3D Printing and Additive Manufactur-
622 ing. <https://doi.org/10.1089/3dp.2022.0012>
- 623 Pakkanen, J., Manfredi, D., Minetola, P., Iuliano, L., 2017a. About the Use of Recycled or
624 Biodegradable Filaments for Sustainability of 3D Printing, in: Campana, G., Howlett,
625 R.J., Setchi, R., Cimatti, B. (Eds.), Springer International Publishing, Cham, pp. 776–
626 785. https://doi.org/10.1007/978-3-319-57078-5_73
- 627 Pakkanen, J., Manfredi, D., Minetola, P., Iuliano, L., 2017b. About the Use of Recycled or
628 Biodegradable Filaments for Sustainability of 3D Printing, in: Campana, G., Howlett,
629 R.J., Setchi, R., Cimatti, B. (Eds.), Sustainable Design and Manufacturing 2017, Smart
630 Innovation, Systems and Technologies. Springer International Publishing, Cham, pp.
631 776–785. https://doi.org/10.1007/978-3-319-57078-5_73
- 632 Pan, Y., Wu, G., Ma, H., Zhou, S., Zhang, H., 2020. Improved compatibility of PET/HDPE
633 blend by using GMA grafted thermoplastic elastomer. Polymer-Plastics Technology and
634 Materials 59, 1887–1898.
- 635 Pearce, J., Qian, J.-Y., 2022. Economic Impact of DIY Home Manufacturing of Consumer
636 Products with Low-cost 3D Printing from Free and Open Source Designs. European
637 Journal of Social Impact and Circular Economy 3, 1–24. <https://doi.org/10.13135/2704-9906/6508>
- 639 Petersen, E., Kidd, R., Pearce, J., 2017. Impact of DIY Home Manufacturing with 3D
640 Printing on the Toy and Game Market. Technologies 5, 45. <https://doi.org/10.3390/technologies5030045>
- 642 Petsiuk, A., Lavu, B., Dick, R., Pearce, J.M., 2022. Waste Plastic Direct Extrusion Hang-
643 printer. Inventions 7, 70. <https://doi.org/10.3390/inventions7030070>
- 644 Pringle, A.M., Rudnicki, M., Pearce, J.M., 2018. Wood Furniture Waste-Based Recycled 3-D
645 Printing Filament. Forest Products Journal 68, 86–95. <https://doi.org/10.13073/FPJ-D-17-00042>
- 647 Raju, M., Gupta, M.K., Bhanot, N., Sharma, V.S., 2019. A hybrid PSO–BFO evolutionary
648 algorithm for optimization of fused deposition modelling process parameters. Journal of
649 Intelligent Manufacturing 30, 2743–2758. <https://doi.org/10.1007/s10845-018-1420-0>
- 650 Rattan, R.S., Nauta, N., Romani, A., Pearce, J.M., 2023. Hangprinter for large scale additive
651 manufacturing using fused particle fabrication with recycled plastic and continuous
652 feeding. HardwareX 13, e00401. <https://doi.org/10.1016/j.johx.2023.e00401>
- 653 Reich, M.J., Woern, A.L., Tanikella, N.G., Pearce, J.M., 2019. Mechanical Properties and
654 Applications of Recycled Polycarbonate Particle Material Extrusion-Based Additive Man-
655 ufacturing. Materials 12, 1642. <https://doi.org/10.3390/ma12101642>
- 656 Rett, J.P., Traore, Y.L., Ho, E.A., 2021. Sustainable Materials for Fused Deposition Modeling
657 3D Printing Applications. Advanced Engineering Materials 23, 2001472. <https://doi.org/10.1002/adem.202001472>

- 659 Romani, A., Rognoli, V., Levi, M., 2021. Design, Materials, and Extrusion-Based Additive
660 Manufacturing in Circular Economy Contexts: From Waste to New Products. *Sustainability* 13, 7269. <https://doi.org/10.3390/su13137269>
- 661
- 662 Roschli, A., Gaul, K.T., Boulger, A.M., Post, B.K., Chesser, P.C., Love, L.J., Blue, F., Borish,
663 M., 2019. Designing for Big Area Additive Manufacturing. *Additive Manufacturing* 25,
664 275–285. <https://doi.org/10.1016/j.addma.2018.11.006>
- 665 Saad, M.S., Nor, A.M., Baharudin, M.E., Zakaria, M.Z., Aiman, A.F., 2019. Optimization of
666 surface roughness in FDM 3D printer using response surface methodology, particle swarm
667 optimization, and symbiotic organism search algorithms. *The International Journal of
668 Advanced Manufacturing Technology* 105, 5121–5137. <https://doi.org/10.1007/s00170-019-04568-3>
- 669
- 670 Salmi, M., Akmal, J.S., Pei, E., Wolff, J., Jaribion, A., Khajavi, S.H., 2020. 3D Printing
671 in COVID-19: Productivity Estimation of the Most Promising Open Source Solutions in
672 Emergency Situations. *Applied Sciences* 10, 4004. <https://doi.org/10.3390/app10114004>
- 673 Santander, P., Cruz Sanchez, F.A., Boudaoud, H., Camargo, M., 2020. Closed loop supply
674 chain network for local and distributed plastic recycling for 3D printing: A MILP-based
675 optimization approach. *Resources, Conservation and Recycling* 154, 104531. <https://doi.org/10.1016/j.resconrec.2019.104531>
- 676
- 677 Savonen, B.L., Mahan, T.J., Curtis, M.W., Schreier, J.W., Gershenson, J.K., Pearce, J.M.,
678 2018. Development of a Resilient 3-D Printer for Humanitarian Crisis Response. *Tech-
679 nologies* 6, 30. <https://doi.org/10.3390/technologies6010030>
- 680 Schirmeister, C.G., Hees, T., Licht, E.H., Mülhaupt, R., 2019. 3D printing of high density
681 polyethylene by fused filament fabrication. *Additive Manufacturing* 28, 152–159. <https://doi.org/10.1016/j.addma.2019.05.003>
- 682
- 683 Sells, E., Smith, Z., Bailard, S., Bowyer, A., Olliver, V., 2009. RepRap: The Replicating
684 Rapid Prototyper - maximizing customizability by breeding the means of production,
685 in: Piller, F.T., Tseng, M.M. (Eds.), *Handbook of Research in Mass Customization and
686 Personalization*. World Scientific, pp. 568–580.
- 687
- 688 Selvam, A., Mayilswamy, S., Whenish, R., 2020. Strength Improvement of Additive Manufac-
689 turing Components by Reinforcing Carbon Fiber and by Employing Bioinspired Interlock
690 Sutures. *Journal of Vinyl and Additive Technology* 26, 511–523. <https://doi.org/10.1002/vnl.21766>
- 691
- 692 Shah, J., Snider, B., Clarke, T., Kozutsky, S., Lacki, M., Hosseini, A., 2019. Large-scale
693 3D printers for additive manufacturing: Design considerations and challenges. *The
694 International Journal of Advanced Manufacturing Technology* 104, 3679–3693. <https://doi.org/10.1007/s00170-019-04074-6>
- 695
- 696 Shirmohammadi, M., Goushchi, S.J., Keshtiban, P.M., 2021. Optimization of 3D printing
697 process parameters to minimize surface roughness with hybrid artificial neural network
model and particle swarm algorithm. *Progress in Additive Manufacturing* 6, 199–215.

- 698 <https://doi.org/10.1007/s40964-021-00166-6>
- 699 Siltaloppi, J., Jähi, M., 2021. Toward a sustainable plastics value chain: Core conundrums
700 and emerging solution mechanisms for a systemic transition. Journal of Cleaner Production
701 315, 128113. <https://doi.org/10.1016/j.jclepro.2021.128113>
- 702 Soares, J., Miguel, I., Venâncio, C., Lopes, I., Oliveira, M., 2021. Public views on plastic
703 pollution: Knowledge, perceived impacts, and pro-environmental behaviours. Journal of
704 Hazardous Materials 412, 125227. <https://doi.org/10.1016/j.jhazmat.2021.125227>
- 705 Taghavi, S.K., Shahrajabian, H., Hosseini, H.M., 2018. Detailed comparison of compatibi-
706 lizers MAPE and SEBS-g-MA on the mechanical/thermal properties, and morphology
707 in ternary blend of recycled PET/HDPE/MAPE and recycled PET/HDPE/SEBS-g-MA.
708 Journal of Elastomers & Plastics 50, 13–35.
- 709 Van de Voorde, B., Katalagarianakis, A., Huysman, S., Toncheva, A., Raquez, J.-M., Duretek,
710 I., Holzer, C., Cardon, L., Bernaerts, K., V, Van Hemelrijck, D., Pyl, L., Van Vlierberghe,
711 S., 2022. Effect of extrusion and fused filament fabrication processing parameters of recy-
712 cled poly(ethylene terephthalate) on the crystallinity and mechanical properties. Additive
713 Manufacturing 50. <https://doi.org/10.1016/j.addma.2021.102518>
- 714 Vaucher, J., Demongeot, A., Michaud, V., Leterrier, Y., 2022. Recycling of Bottle Grade
715 PET: Influence of HDPE Contamination on the Microstructure and Mechanical Per-
716 formance of 3D Printed Parts. Polymers 14, 5507. <https://doi.org/10.3390/polym14245507>
- 717 Verma, N., Awasthi, P., Gupta, A., Banerjee, S.S., 2023. Fused Deposition Modeling of
718 Polyolefins: Challenges and Opportunities. Macromolecular Materials and Engineering
719 308, 2200421. <https://doi.org/10.1002/mame.202200421>
- 720 Wijnen, B., Sanders, P., Pearce, J.M., 2018. Improved model and experimental validation
721 of deformation in fused filament fabrication of polylactic acid. Progress in Additive
722 Manufacturing 3, 193–203. <https://doi.org/10.1007/s40964-018-0052-4>
- 723 William, L.J.W., Koay, S.C., Chan, M.Y., Pang, M.M., Ong, T.K., Tshai, K.Y., 2021. Re-
724 cycling Polymer Blend made from Post-used Styrofoam and Polypropylene for Fuse De-
725 position Modelling. Journal of Physics: Conference Series 2120, 012020. <https://doi.org/>
726 [10.1088/1742-6596/2120/1/012020](https://doi.org/10.1088/1742-6596/2120/1/012020)
- 727 Woern, A.L., McCaslin, J.R., Pringle, A.M., Pearce, J.M., 2018. RepRapable Recyclebot:
728 Open source 3-D printable extruder for converting plastic to 3-D printing filament. Hard-
729 wareX 4, e00026. <https://doi.org/10.1016/j.ohx.2018.e00026>
- 730 Wong, J.Y., 2015. Ultra-Portable Solar-Powered 3D Printers for Onsite Manufacturing of
731 Medical Resources. Aerospace Medicine and Human Performance 86, 830–834. <https://doi.org/10.3357/AMHP.4308.2015>
- 733 Zander, N.E., Gillan, M., Burckhard, Z., Gardea, F., 2019. Recycled polypropylene blends
734 as novel 3D printing materials. Additive Manufacturing 25, 122–130. <https://doi.org/10.1016/j.addma.2018.11.009>
- 736 Zander, N.E., Gillan, M., Lambeth, R.H., 2018. Recycled polyethylene terephthalate as a

- 737 new FFF feedstock material. Additive Manufacturing 21, 174–182. <https://doi.org/10.1016/j.addma.2018.03.007>
- 738
- 739 Zhang, Y., Wang, S., Ji, G., 2015. A Comprehensive Survey on Particle Swarm Optimization
740 Algorithm and Its Applications. Mathematical Problems in Engineering 2015, e931256.
741 <https://doi.org/10.1155/2015/931256>
- 742 Zhong, S., Pearce, J.M., 2018. Tightening the loop on the circular economy: Coupled dis-
743 tributed recycling and manufacturing with recyclebot and RepRap 3-D printing. Re-
744 sources, Conservation and Recycling 128, 48–58. <https://doi.org/10.1016/j.resconrec.2017.09.023>
- 745